

Theoretical and Experimental Investigation on Back-scattered Low Energy Gamma Radiation from Different Metals

A.Pazirandeh and N.Sobhkhiz

Physics Department, University of Tehran, Tehran Iran

Abstract

Gamma-ray and X-ray are powerful tools for analysis of internal material micro-structure. The technique is based on studying the leakage spectrum. Two basic phenomena are involved in this work, namely photo-electric effect and Compton scattering. We derived the fundamental equations to calculate four components contributed in building up the leakage spectrum, which are Compton-Compton, Rayleigh-Compton, Compton-Rayleigh and Rayleigh-Rayleigh scattering. Results of our calculation and measurements for aluminum target showed very good agreement.

Keywords: Compton scattering, Rayleigh scattering, Double scattering, Albedo spectrum, Coherent and incoherent scattering

1. INTRODUCTION

Quantum understanding of surface and internal structure of materials is a key role in material behavior in physical and chemical interactions. X-ray and low gamma radiation are powerful tools that can be exploited to study momentum distribution of electrons, electron density, structural irregularities, and defects. The back-scatter low energy gamma rays reveal much information. By detailed analysis of multi-scattered gamma leakage spectra or albedo gamma flux a great deal of information are obtained.

To study a single type atom property in a sample through the scattered spectrum analysis, multiple scattering creates error and misinterpretation. Therefore, the spectrum has to be corrected for contributions from multiple scattering. The objective of this study was to treat the problem of multiple scattering primarily by transport theory and subsequently by carrying out the experimental measurement to validate the theoretical model.

2. THEORETICAL DERIVATION

The general form of transport equation is derived from the difference between number of photons with definite energy and direction emerging from a specific point entering a cylindrical volume and those outgoing from it. The net rate of photon flux, having a finite energy, leaving the cylinder at a specific direction is equal to (Fig. 1):

$$f(r + dl, \omega) dA - f(r, \omega) dA \dots \dots \dots (1)$$

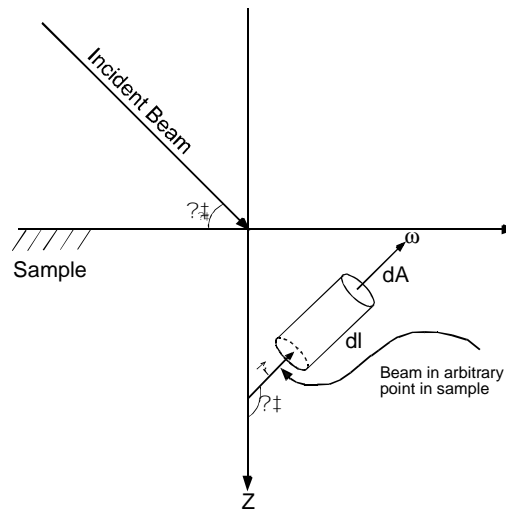


Figure 1 - Schematic Diagram of gamma Interaction in Volume Element.

Using Taylor expansion, equation(1) is written as:

$$f(r + dl, \omega) dA - f(r, \omega) dA = dl \nabla f(r, \omega) dA \dots \dots \dots (2)$$

Based on the continuity theorem, three terms contribute the gamma flux in the volume element, which are as following:

1. Absorption of photons in photoelectric process, change in direction and energy of photons in Compton scattering.

The contribution of the directional mono-energetic gamma flux outside the volume element is equal to:

$$-f(r, \omega) dA dl$$

summing up all the components, the total emerging gamma flux is obtained as:

$$f = f^{(0)} + f^{(1)} + f^{(2)} + \dots \tag{5}$$

Since each component is defined as a kernel, K, which is less than one and the higher order terms of the series diminish, therefore, we considered only three terms. With using Kronecker delta function the equation is written as:

$$f^{(n)}(z, \omega, \Omega) = \int_0^z f^{(n-1)}(z', \omega', \Omega') K(z, \omega, \Omega; z', \omega', \Omega') u(z) dz' \tag{6}$$

After lengthy mathematics (Murray 1974; Gilmore & Hemingway 1995), the general flux component inside the sample was obtained as:

$$f^{(n)}(z, \omega, \Omega) = \frac{1}{2} \left\{ \frac{[1 - \text{sgn}(\omega)]}{2} \exp\left(-\frac{z}{\lambda}\right) \int_0^z \exp\left(-\frac{z'}{\lambda}\right) * \int_0^{z'} K(z, \omega, \Omega; z', \omega', \Omega') f^{(n-1)}(z', \omega', \Omega') dz' \right. \\ \left. + \frac{[1 + \text{sgn}(\omega)]}{2} \int_0^z \exp\left(-\frac{z'}{\lambda}\right) \int_0^{z'} K(z, \omega, \Omega; z', \omega', \Omega') f^{(n-1)}(z', \omega', \Omega') dz' \right\} \tag{7}$$

Now we could evaluate the partial intensity i.e., number of photons emerging from surface area of the sample at right angle, per unit area, per unit time, per unit wavelength on the direction ω at $z = 0$ as:

$$I^{(n)}(\omega) = \lambda f^{(n)}(0, \omega, \Omega) \tag{8}$$

$I^{(n)}$ yields complete information about emerging gamma ray angular distribution.

Since the energy of Ir-192 gamma ray is rather low (316 Kev, 468 Kev), therefore photoelectric effect is predominant phenomenon and there will be only two or three multi-scattering of photo-peak gamma ray inside the sample. As such we solved the problem only for double scattering.

A – Rayleigh – Rayleigh Scattering

By introducing following Rayleigh scattering kernel in equation (7):

$$K_R(\vec{k}, \vec{k}') = \frac{F^2(\vec{k}, \vec{k}', \mathbf{z})}{Z} \tag{12}$$

following equation is obtained (Veigele *et.at.*, 1966):

$$I_{R^2}^{(2)}(\vec{k}, \vec{k}') = \frac{1}{Z^2} \int_0^{2\pi} \int_0^{2\pi} \frac{F^2(\vec{k}, \vec{k}', \mathbf{z}) F^2(\vec{k}, \vec{k}', \mathbf{z})}{\dots} * F^2(\vec{k}, \vec{k}', \mathbf{z}) * F^2(\vec{k}, \vec{k}', \mathbf{z}) \tag{13}$$

The Rayleigh-Rayleigh intensity is discrete and added with Rayleigh peak.

B – Compton – Compton Scattering

By introducing Compton kernel given below in equation(7) :

$$K_C(\vec{k}, \vec{k}') = \frac{1}{\epsilon} \frac{K_{KN}(\vec{k}, \vec{k}') S(\vec{k}, \vec{k}', \mathbf{z})}{\dots}$$

following equation is obtained:

$$I_{C^2}^{(2)}(\vec{k}, \vec{k}') = \frac{1}{\epsilon^2} \frac{u(\vec{k}, \vec{k}')}{[(1+\epsilon^2)(1+\epsilon'^2) (\dots)]^{1/2}} * \frac{K_{KN}(\vec{k}, \vec{k}') K_{KN}(\vec{k}, \vec{k}') S(\vec{k}, \vec{k}', \mathbf{z}) S(\vec{k}, \vec{k}', \mathbf{z})}{\dots} * S(\vec{k}, \vec{k}', \mathbf{z}) S(\vec{k}, \vec{k}', \mathbf{z}) \tag{14}$$

C – Rayleigh - Compton Scattering

$$\begin{aligned}
 & \mathbf{I}_{R+C}^{(2)} = \frac{1}{z} \mathbf{A}(\mathbf{k}, \omega) \mathbf{K}_{KN}(\mathbf{k}, \omega) \mathbf{S}(\mathbf{k}, \omega, \mathbf{z})^* \\
 & * \left\{ \frac{1}{z} \cdot \frac{1}{|\mathbf{k}|} \cdot \frac{1}{|\mathbf{k}'|} \cdot \frac{u(\mathbf{k}, \omega)}{[(1-\beta^2)(1-\beta^2)(a^2 - \beta^2)]^{1/2}} \right\} \\
 & * \int_{k_1}^2 [1 - (\beta \cos \theta)^2] F^2(\mathbf{k}, \omega, \mathbf{z}) \\
 & * \left\{ \frac{1}{z} \cdot \frac{1}{|\mathbf{k}|} \cdot \frac{1}{|\mathbf{k}'|} \cdot \frac{u(\mathbf{k}, \omega)}{[(1-\beta^2)(1-\beta^2)(a^2 - \beta^2)]^{1/2}} \right\} \\
 & * \int_{k_1}^2 [1 - (\beta \cos \theta)^2] F^2(\mathbf{k}, \omega, \mathbf{z})
 \end{aligned}$$

$$\begin{aligned}
 & \max(0, a - D) \dots \dots \dots \min(1, a - D) \\
 & \min(0, a + D) \dots \dots \dots \max(1, a + D) \\
 & a - \frac{b}{e} \dots \dots \dots D \sqrt{(1 - \beta^2)(1 - a^2)}^{1/2} \\
 & \arccos \left[\frac{a \beta \cos \theta}{[(1 - \beta^2)(1 - a^2)]^{1/2}} \right] \\
 & 2 \dots \dots \dots (\dots)
 \end{aligned}$$

The Rayleigh-Compton intensity is continuous and its wavelength spectrum extends from λ_0 to $\lambda_c + 2 \lambda_c$ as shown in Figure 3.

$$\begin{aligned}
 & \min(0, a - D) \dots \dots \dots \min(1, a - D) \\
 & \min(0, a - D) \dots \dots \dots \max(1, a - D) \\
 & a > 1 \Rightarrow \frac{a - D}{a} \dots \dots \dots D \sqrt{[(1 - \sigma^2)(1 - a^2)]^{1/2}} \\
 & \arccos\left[\frac{a - D}{a}\right] \\
 & Z_2^{(2)} \dots \dots \dots Z_1^{(2)} \dots \dots \dots
 \end{aligned}$$

The integration performed on the basis of Romberg (Nakamura, 1991) generalized form for improper integrals. A computer program based on the above equations was prepared in PASCAL to calculate the out-flux from the sample.

3. EXPERIMENTAL SETUP

The experiment was carried out using a 1Ci Iridium-192 source housed in a lead shield as shown in Figure 4. Iridium-192 emits two gamma rays of 316.5 Kev and 468.06 Kev. The source gamma was collimated through a 20-cm long beam hole of 1.0cm in diameter. The target surface in question was placed at 45⁰ angle to the beam. The gamma-rays were counted on a HPGe detector in a heavy shield placed in such a way that the crystal axis was at right angle to the source beam, i.e., at 45⁰ angle to the sample surface. A collimator with 1.0cm beam hole was placed in front of the crystal.

The counting apparatus comprised of the detector, preamplifier, amplifier, power supplies and a computer based multi-channel analyzer (MCA).

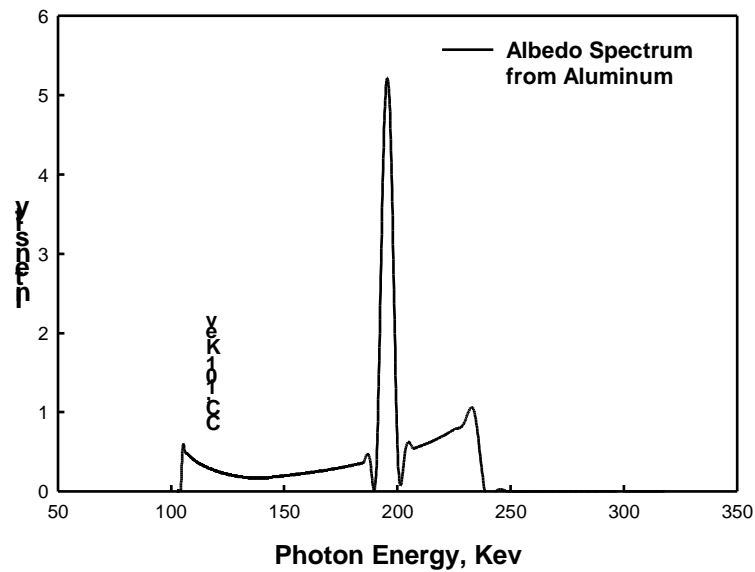


Figure 5 - Single Scattering of Compton, Rayleigh and Double Scattering of Compton-Compton, Compton-Rayleigh, Rayleigh-Compton, and Rayleigh-Rayleigh

of Ir-192, 316.5 and 486.06 Kev, were calculated and summed up. Figure 7 shows the summed spectrum. There is a very good agreement between theoretical calculation (Fig. 7) and experimental measurement (Fig. 6).

In fact the minor difference between calculated and measured spectra firstly emanates from other photo-peaks with smaller fractions in the decay scheme of Ir-192. Another source of difference is due to the fact that, in our calculation we have not considered the electron motion as well as detector efficiency, which are in fact responsible for Doppler broadening in measured spectrum. That is why peaks in calculated spectrum are narrower than measured one. In fact the aim of this experiment was to position exactly the peaks in the spectrum.

In experiments of Compton profile that lead to the determination of electron momentum distribution, multiple scattering is considered as a destructive agent in the spectrum shaping. In order to obtain the pure

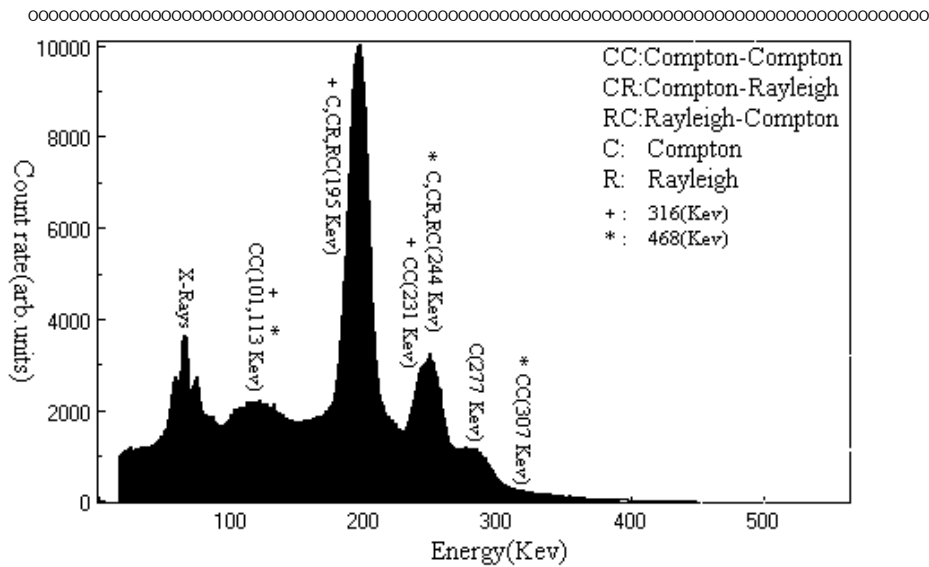


Figure 6 - Measured Albedo Spectrum of Al Target excited with 316 Kev Ir-192 Source at Incident Angle of 45 and take-off Angle of 135.

spectrum due to electron momentum distribution, the contribution of multiple scattering has to be eliminated. Therefore, we should know the exact position of peaks of multiple scattering for better spectrum analysis. In fact we have identified the position of peaks and the contribution of each component.

As it is seen, transport theory takes into account the lower terms of multiple scattering in calculating the total spectrum. Therefore, we could estimate the contribution of each scattering type from individual atom in the albedo spectrum. This results show that we can obtain the intensity of multiple scattering for different directional and polar angles. As such, we shall be able to determine an angle that the contribution of multiple scattering will be minimal and will have minimum effect on albedo spectrum.

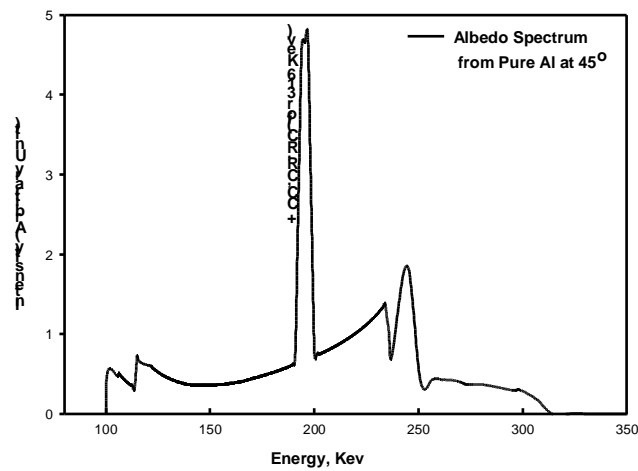


Figure 7 - Sum of all single and double scattering for two photo-peaks of 316.06 and 486.5 KeV. For comparison see Figure 5.

ACKNOWLEDGMENTS

The authors would like to thank Mr. Abdol-Reza Ghahremani, Industrial Radioisotope Production Section, Nuclear Research Center, AEOI, for providing Ir-192 source.

REFERENCES

- Fernandez J.E., Molinaro V.G., and Sumini H., (1989) *Effect of the X-ray scattering anisotropy of the diffusion of photons in the fame of the tranport theory*, Nucl. Inst. & Methods A-280, 212.
- Gilmore Gordon, Hemingway John O., *Practical Gamma-ray spectrometry*, Wiley, 1995.
- Murray R., *Fourier Analysis*, McGraw-Hill Publishing Co., 1974.
- Nakamura S., *Applied Numerical Methods with Software*, Prentice-Hall Int. 1991.
- Veigle W.J., Tracy P.T., and Henry E.M., (1966) *Coherent and incoherent Atomic form factors*, Am.J. Phys. **34**, 1116.

